Progress In Electromagnetics Research M, Vol. 32, 43–55, 2013

SINGLE-NANOWEB SUSPENDED TWIN-CORE FIBER FOR OPTICAL SWITCHING

Xiaowei Ma and Daru Chen*

Institute of Information Optics, Zhejiang Normal University, Jinhua 321004, China

Abstract—A novel suspended twin-core fiber (STCF) based on a single-nanoweb structure for optical switching is proposed. The single-nanoweb structure of the STCF is an ultrathin glass membrane (nanoweb) suspended in air and adhered to the inner ring of a glass fiber capillary, which substantially provides a built-in transducing mechanism to boost the pressure-induced index change in the fiber core region of the STCF. Two fiber cores locate symmetrically in the center of the nanoweb, resulting to the mode coupling for the guiding light in the STCF. Optical and mechanical properties of the proposed STCFs under different force are numerically investigated. Optical switching based on the STCF is achieved by controlling the force applied to the STCF. Our simulations show that optical switching from one core to the other in the STCF is realized based on a low switching force of only 8 N. The performances of the optical switching based on STCFs with different structure parameters are presented.

1. INTRODUCTION

All-optical networks (AON) [1, 2], which have attracted considerable attentions for their manageability [3, 4], transparency [5–8], and flexibility [9–13], are considered to be the candidates for the future communication networks invariably by scholars. As an important supporting technology of optical communication systems, optical switching is taken account for the key-enabling function for the deployment of the developing all-optical networks and many efforts have been made on trying to accomplish it. As far as we know, the technologies to realize optical switching include optical micro-electro-mechanical systems (MEMS)-based switching [14–16], thermal

Received 20 May 2013, Accepted 6 July 2013, Scheduled 15 July 2013

* Corresponding author: Daru Chen (daru@zjnu.cn).

optical switching [17, 18], electro-optic switching [19–21], opto-optical switching [22–25], acousto-optic switching [26] technologies and other technologies integrating some of them [27]. However, much of the optical switches are still predominantly performed electrically in recent applications. With the emergence and development of the microstructure fiber (MSF) which has shown a great success to achieve unique properties such as high birefringence [28–36], flattened dispersion [37–40], large negative dispersion [41, 42], high nonlinearity [43, 44], endless single mode [45] and so on, there emerges a new opportunity for the exploration of optical switching technology that it is possible to make the optical fiber be an optical switch. Recently, a type of nanomechanical optical fiber [46] has been proposed and demonstrated, which has two fiber cores independently suspended within the fiber. Based on sub-micron mechanical movements, the nanomechanical fiber shows the optical switching between the two fiber cores, which clearly shows the possibility to achieve an optical switching device with advantages such as fiber compatibility, compared with the traditional optical switches. However, the demonstrated nanomechanical optical fiber in Ref. [46] has a complex structure and needs to break the fiber cladding to achieve the mechanical movements of the fiber cores, which limits its practical applications.

In this paper, we propose a suspended twin-core fiber (STCF) based on a single-nanoweb structure for optical switching. It utilizes an ultrathin silica lamina suspended in air and attached to the inner wall of a glass fiber capillary, and there are two solid fiber cores near the central part of the nanoweb. The force applied to the proposed STCF is used to achieve optical switching. The mode coupling between the two fiber cores is sensitive to the pressure-induced index change, which provides a one-to-one correspondence (within a half period) between the force and the transmittivity of one core into which the broadband light is injected. The performances of optical switches based on STCFs with different structure parameters are presented.

2. STRUCTURE AND PERFORMANCE

The geometry structure of the cross-section of the proposed STCF is shown in Figure 1. There is an ultrathin glass membrane suspended in air and attached to the inner wall of a glass fiber capillary. The external diameter of the capillary is (D), in our simulations, which is kept being a constant of 125 μm. The radius of the capillary's inner ring is (R). Figure 1(b) shows the enlarged view of the center structure of the nanoweb with the twin cores. The thickness of the nanoweb is (d). The radius of the twin cores is (r). The distance between the centers of

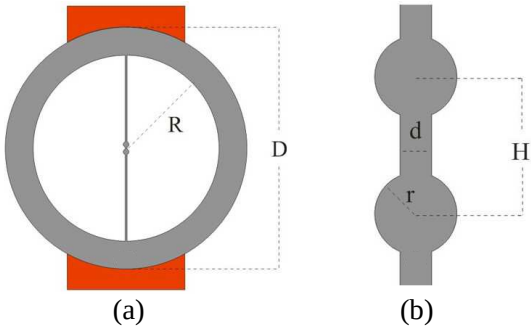

Figure 1. (a) Cross-section of the proposed STCF with a fiber clamp (the red part). (b) Enlarged view of the twin-core region of the proposed STCF.

the two fiber cores is (H). We use a full-vector finite-element method (FEM) to analyze the influence of the force applied to the proposed STCF and also investigate the guided modes.

In the pressure analysis, two pieces of iron are adopted to imitate a fiber clamp in actual applications, and placed on the direction of the nanoweb. When the fiber clamp is under force, the force applied to the STCF will lead to not only the pressure-induced refractive index change, but also the pressure-induced structure deformation. In terms of the contribution to the light guiding and mode coupling, the role of the pressure-induced structure deformation is so small [47] that we usually ignore it. According to the well-known photoelastic effect, the refractive index of the silica under the force is given by the equations [48]

$$n_x = n_0 - C_1\sigma_x - C_2\left(\sigma_y + \sigma_z\right) \quad (1)$$

$$n_y = n_0 - C_1\sigma_y - C_2\left(\sigma_x + \sigma_z\right) \quad (2)$$

$$n_z = n_0 - C_1\sigma_z - C_2\left(\sigma_x + \sigma_y\right) \quad (3)$$

and the pressure-induced refractive index change is

$$\Delta n_x = n_x - n_0 = -C_1\sigma_x - C_2\left(\sigma_y + \sigma_z\right) \quad (4)$$

$$\Delta n_y = n_y - n_0 = -C_1\sigma_y - C_2\left(\sigma_x + \sigma_z\right) \quad (5)$$

$$\Delta n_z = n_z - n_0 = -C_1\sigma_z - C_2\left(\sigma_x + \sigma_y\right) \quad (6)$$

where σ_x, σ_y and σ_z are the stress components, and $C_1 = 6.5 \times 10^{-13}\,\mathrm{m}^2/\mathrm{N}$ and $C_2 = 4.2 \times 10^{-12}\,\mathrm{m}^2/\mathrm{N}$ are the stress-optic coefficients of pure silica. Thus, through the FEM analysis we can know the refractive index change of the silica under different force. Note that, in the process of calculations, z-direction is usually ignored since it almost makes no difference to the polarized mode of the optical fiber.

When a force of 1 N is applied to a 10-cm STCF with parameters of $D = 125\,\mu m$, $R = 50\,\mu m$, $d = 1\,\mu m$, $r = 1\,\mu m$, and $H = 3\,\mu m$, the calculated σ_y in the STCF is shown in Figure 2(a). Note that the calculated σ_x is much smaller than σ_y in the twin-core region and it is 0 in the rest part of the nanoweb, thus it is ignored for the pressure-induced index change. One can very clearly see the amplification effect of the proposed structure, that is to say, a force of 1 N applied to the STCF results to a high stress up to about 6.3 Mpa in the nanoweb of the STCF. According to Eqs. (4) and (5), it's easy to describe the distribution of the pressure-induced refractive index change along the y direction, which is shown in Figure 2(b). For example, the pressure-induced index change is $\Delta n_x = 20.2 \times 10^{-6}$ and $\Delta n_y = 3.1 \times 10^{-6}$ in the center of the fiber cores, which shows that the x-polarized light has a stronger response to the force applied to the STCF.

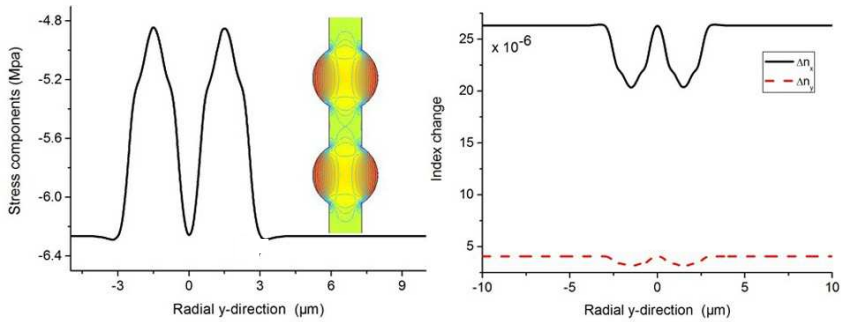

Figure 2. (a) Distribution of the principal stress component of σ_y in the radial y-direction and (b) pressure-induced refractive index change (Δn_x and Δn_y in the radial y-direction) of the STCF with parameters of $D = 125\,\mu m$, $R = 50\,\mu m$, $d = 1\,\mu m$, $r = 1\,\mu m$, and $H = 3\,\mu m$.

It is mentioned above that the guiding light in the proposed STCF will be influenced by the pressure-induced refractive index change. To make it unequivocal, we simulate the guiding modes in the twin-core region and acquire the effective refractive indices of the even mode and the odd mode. Figures 3(a) and (b) show the mode profiles of the electric field for the even mode and the odd mode, respectively, and meanwhile describe their normalized electric field distribution along the y direction. Note that the operation wavelength λ is set at 1550 nm, and a 10-cm STCF with parameters of $D = 125\,\mu m$, $R = 50\,\mu m$, $d = 1\,\mu m$, $r = 1\,\mu m$, and $H = 3\,\mu m$ is employed. The calculated effective refractive indices of the even mode and the odd mode are $n_e = 1.36493$ and $n_o = 1.36122$. According to the mode coupling

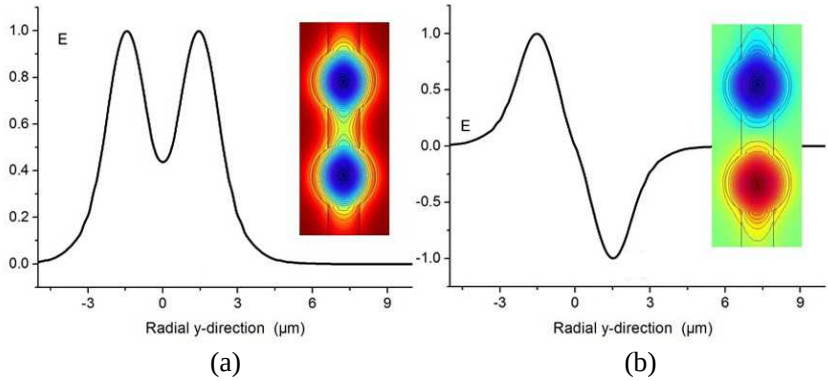

Figure 3. Mode profiles and electric field distribution along the radial y-direction for (a) the even mode and (b) the odd mode of the STCF at the wavelength of 1550 nm.

theory, the optic power transferred from one fiber core to the other fiber core after a length Z along the STCF is given by [49]

$$p(\lambda, Z) = \sin^2\left(|n_e - n_o|\, Z \cdot \pi/\lambda\right) = \sin^2(\Delta n_{eo} Z \cdot \pi/\lambda) \tag{7}$$

and the coupling length is given by [49]

$$L_c = \lambda/\left(2\,|n_e - n_0|\right) \tag{8}$$

Note that the coupling strength is usually expressed by the coupling length or the coupling coefficient. The relation between them also has shown in [49].

$$L_c = \lambda/4k_{12} \tag{9}$$

According to Eqs. (7) and (8), we can get a function of the optical transmittivity dependent on Z and L_c

$$p(Z, L_c) = \sin^2(Z \cdot \pi/2L_c) \tag{10}$$

When the x-polarized laser light with the wavelength of 1550 nm is injected into one fiber core of the STCF without applied force, we can calculate transmittivity for another fiber core of the STCF according to Eq. (9). Figure 4 shows transmittivity when the length of the STCF is in the range around 10 cm. One can see that after only 0.22 mm, the light of this core can be transferred to the other one completely. Therefore we can use the length of its integral multiple to initialize the optical switching device.

Figure 5 shows the (x-polarized) transmission of the STCF with the length of 9.96 cm and 5.03 cm at a force range from 0 to 950 N. Here, we define a switching force (ΔF) that is a force applied to the STCF to switch guided light from one fiber core to the other. One can distinctly

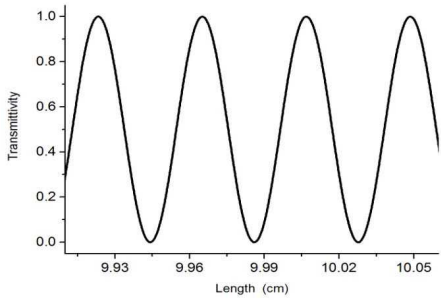

Figure 4. Distribution of transmittivity (x-polarized) along the length of the STCF with parameters of $D = 125\,\mu\text{m}$, $R = 50\,\mu\text{m}$, $d = 1\,\mu\text{m}$, $r = 1\,\mu\text{m}$, and $H = 3\,\mu\text{m}$.

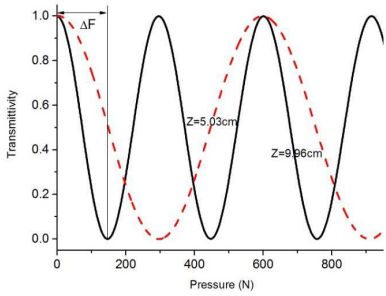

Figure 5. X-polarized transmission of the STCF with the length of 9.96 cm (black solid curve) or 5.03 cm (red dashed curve).

see that for the STCF with same structure parameters, longer the fiber is, smaller the switching force is needed, in the case of the incident light with a fixed wavelength. And the switching force of the STCF with the length of 9.96 cm is 148 N. Mechanical strength of fiber has been commonly mentioned in the experiments of fiber pressure sensing [50].

For the given length of the proposed STCF, small ΔF is expected to achieve optical switching in practical applications, which actually pushes us to design a STCF with high force sensitivity. Therefore, here we investigate STCFs with different parameters for optical switching. Note that, in the following discussions, a 10-cm STCF with parameters of $D = 125\,\mu\text{m}$, $R = 50\,\mu\text{m}$, $d = 1\,\mu\text{m}$, $r = 1\,\mu\text{m}$, and $H = 3\,\mu\text{m}$ is used as the reference for which ΔF of 148 N is needed to achieve optical switching.

Firstly, we change the radius of the inner ring of the glass capillary when other parameters of the STCF are fixed. The relationship between the switching force ΔF and the radius R is shown in Figure 6. Note that all STCFs are with the same length of 10 cm for the calculated results in Figure 6. Obviously, a STCF with a larger radius R has a smaller switching force ΔF. This can be understood due to the fact the larger air hole of the STCF is more sensitive to the applied force. The principle is similar with the special MSFs [51] with side holes which provide an internal amplification mechanism to enhance the force sensitivity. However, in practical applications, R is limited by the physical strength of the fibers. Secondly, according to the contrast of several different structures, we deploy the exploration of the role of the distance H of the twin cores. Figure 7 shows that optical switching will be more difficult when the distance of the twin

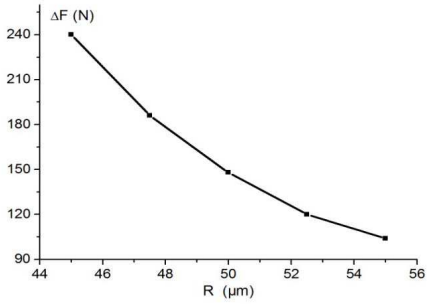

Figure 6. Switching force for optical switching of a 10-cm STCF under the different values of R.

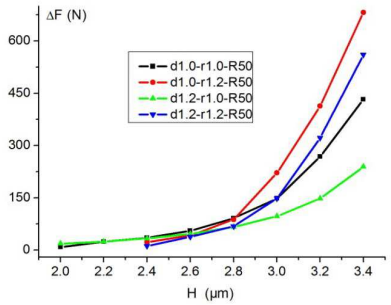

Figure 7. Switching force for optical switching of a 10-cm STCF under the different values of H.

cores is widening, that is due to the fact that the larger distance H results to weak mode coupling between the twin cores. The size of fiber cores also influences the property of the STCF for optical switching. For a given STCF, when we change the size of fiber cores within a certain range, there is a maximum value for ΔF which is shown in Figure 8. When the twin cores are most close to each other (i.e., they are tangent), the corresponding ΔF will be the minimum. Meanwhile, when r becomes smaller, a smaller ΔF can also be achieved, which indicates the smaller r is preferred. Here we can find two effects for the size of the fiber cores and the mode coupling. A larger r will enhance the mode overlapping of the twin cores since they are closer to each other. While the fiber core with a small r will result to weak confinement of the mode light, and also strong mode coupling of the twin cores. Thus a suitable value of r should be chosen for practical applications of the STCF when considering the light confinement and sensitivity for optical switching. Likewise, similar behaviour can be seen for the parameter d. Figure 9 shows the switching force ΔF for a 10-cm STCF with different thickness (d) of the nanoweb when other parameters are fixed. It can come to be a conclusion that the optimized thickness (d) will lead to a minimum value of the switching force ΔF. When d turns to be thin, for a given force applied to the STCF, pressure-induced index change of the twin cores becomes larger due to the built-in transducing mechanism. However, the thickness (d) of the nanoweb will also influence the mode coupling, that is, the thin nanoweb will lead to a weak mode coupling of the twin cores since there is more air instead of silica material between the twin cores. Thus, we can understand the thickness (d) can be optimized to achieve minimum switching force ΔF. Generally, parameters of the STCF for

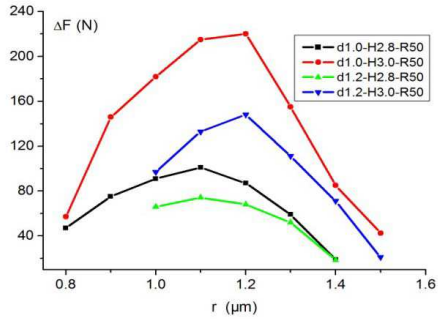

Figure 8. Switching force for optical switching of a 10-cm STCF under the different values of r.

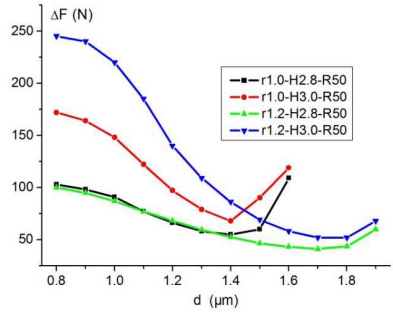

Figure 9. Switching force for optical switching of a 10-cm STCF under the different values of d.

optical switching can be optimized to achieve a low switching force. Under the guidance of the above-mentioned discussions, we find the optimized structure of the STCF with parameters of $D = 125\,\mu\text{m}$, $R = 50\,\mu\text{m}$, $d = 1\,\mu\text{m}$, $r = 1\,\mu\text{m}$, and $H = 2\,\mu\text{m}$ for optical switching, and the calculated switching force is $\Delta F = 8\,\text{N}$. Note that we choose a fiber size same as the single mode fiber and a reasonable radius R here, and the switching force can be much smaller if we use a much larger STCF with a larger radius R.

3. DISCUSSION AND CONCLUSION

The recently designed nanomechanical optical fiber [46] and the proposed STCF are actually two kinds of microstructured optical fibers with a dual-nanoweb structure and a single-nanoweb structure, respectively. The proposed STCF shows several advantages. Firstly, the single-nanoweb structure is relatively simple which benefits the fiber fabrication process. Such as easily controlling the size of the twin cores and the distance between them. Special measures should be taken to control the distance of the two fiber cores for nanomechanical optical fiber with the dual-nanoweb structure in the fabrication process. Secondly, optical switching can be achieved by controlling the force applied to the external surface of the STCF, but one should break the fiber cladding of the dual-nanoweb fiber to achieve optical switching. The STCF is used as the optical switch by simply add suitable fiber clamp. Thirdly, for the proposed STCF, optical switching is achieved based on the pressure-induced index change which essentially

has advantages such as high response speed and high repeatability, compared with optical switch based on mechanical movement of the dual-nanoweb fiber. There is some research work on the fiber-optic vibration sensors based on the photoelastic effect of the fiber which indicates that the response frequency of pressure applied on the fiber can at least up to 3000 Hz. According to the successful optical switching of the nanomechanical optical fiber [46] and the load force test in the experiment of fiber pressure sensing [50], we can believe that the STCF can withstand 8 N to achieve optical switching without breaking the structure. Of course, since there is a thin structure in the proposed STCF, further experimental research is still needed to make sure how much force the STCF can bear.

In conclusion, we have proposed and investigated a novel STCF based on a single-nanoweb structure, which can be used as an optical switch. Optical and mechanical properties of the proposed STCFs under different force have been numerically investigated. By analyzing the mode coupling between the twin cores, we reveal the rule of the STCF's parameters for optical switching and indicate the optimized method for achieving an optical switch with low switching force. Finally, we also discuss the advantages of the proposed STCF compared with the early reported dual-nanoweb fiber.

ACKNOWLEDGMENT

This work was supported in part by the National Natural Science Foundation of China under project (No. 61007029), Projects of Zhejiang Province (No. 2011C21038 and No. 2010R50007) and the Program for Science and Technology Innovative Research Team in Zhejiang Normal University.

REFERENCES

1. Berthold, J., A. A. M. Saleh, L. Blair, and J. M. Simmons, "Optical networking: Past, present, and future," *J. Lightwave Technol.*, Vol. 26, 1104–1118, 2008.
2. Saleh, A. A. M. and J. M. Simmons, "All-optical networking-evolution, benefits, challenges, and future vision," *Proc. of IEEE*, Vol. 100, 1105–1117, 2012.
3. Wang, X., Y. Ji, L. Bai, H. Xing, and J. Fu, "Design and experimental demonstration of network coding in all-optical multicast networks," *Proc. of IC-NIDC*, 500–504, 2009.
4. Rejeb, R., M. S. Leeson, and R. J. Green, "Fault and attack

management in all-optical networks," *IEEE Commun. Mag.*, Vol. 44, 79–86, 2006.

5. Payne, D. B. and J. R. Stern, "Transparent single-mode fiber optical networks," *J. Lightwave Technol.*, Vol. 4, 864–869, 1986.
6. Marciniak, M., "IP/optical networks: The impact of optical transparency," *LFNM*, 25–36, Kaharkiv, Ukraine, 2001.
7. Moghaddam, E. S., J. Tapolcai, and D. Mazroa, "Physical impairment of monitoring trails in all optical transparent networks," *Int. Congress on Ultra Modern Telecommunications and Control Systems and Workshops (ICUMT)*, 1–7, ISBN 978-963-8111-77, 2011.
8. Krishnan, S. and A. Borude, "Security issues in all-optical networks," *2011 Annual SRII Global Conference*, 790–794, 2011.
9. Zhang, J. and Y. Zhao, "Routing and spectrum assignment problem in three-C-aware dynamic flexible optical networks," *Proc. of SPIE-OSA-IEEE Asia Communications and Photonics*, Vol. 8310, 1–7, 2011.
10. Cuda, D., R. M. Indre, E. L. Rouzic, and J. Roberts, "Building a low-energy transparent optical wide area network with 'multipaths'," *J. Opt. Commun. Netw.*, Vol. 5, 56–67, 2013.
11. Yan, L., A. E. Willner, X. Wu, A. Li, A. Bogoni, Z. Y. Chen, and H. Y. Jiang, "All-optical signal processing for ultrahigh speed optical systems and networks," *J. Lightwave Technol.*, Vol. 30, 3760–3770, 2012.
12. Johansson, S., M. Lindblom, P. Granestrand, B. Lagerstrom, and L. Thylen, "Optical cross-connect system in broad-band networks: System concept and demonstrators description," *J. Lightwave Technol.*, Vol. 11, 688–694, 1993.
13. Simmons, J. M., *Optical Network Design and Planning,* Springer-Verlag, New York, 2008.
14. Borobic, B., C. Hong, A. Q. Liu, L. Xie, and F. L. Lewis, "Control of a MEMS optical switch," *43rd IEEE Conf. Decision and Control*, 3039–3044, 2004.
15. Owusu, K. O., F. L. Lewis, B. Borovic, and A. Q. Liu, "Nonliner control of a MEMS optical switch," *45rd IEEE Conf. Decision and Control*, 597–602, 2006.
16. Abdulla, S. M. C., L. J. Kauppinen, M. Dijkstra, E. Berenschot, M. J. de Boer, R. M. de Ridder, and G. J. M. Krijnen, "Mechano-optical switching in a MEMS integrated photonic crystal slab waveguide," *IEEE 24th Int. Conf. on Micro Electro Mechanical Systems*, 9–12, 2011.

17. Li, M. G., D. J. Tebben, M. J. Soulliere, S. Hilbert, M. Zhao, I. Lelic, D. G. Hoefer, M. Gauland, V. Kaliniouk, L. Guiziou, J.-M. Jouanno, and R. E. Wagner, "Two-fiber optical channel shared protection ring with 4×4 thermal-optic switches," *Proc. OFC 2001*, Vol. 2, 228–229, 2001.
18. Perron, D., M. Wu, C. Horvath, D. Bachman, and V. Van, "All-optical switching in SU-8 conductor-gap-dielectric plasmonic microring resonator using thermal nonlinearity," *Proc. Quantum Electronics and Laser Science Conf.*, 1–2, Baltimore, MD, 2011.
19. Li, C. and A. W. Poon, "Silicon electro-optic switching based on coupled-microring resonators," *Conf. on Lasers and Electro-Optics (CLEO)*, 1–2, 2007.
20. Ghafoori-Fard, H., M. J. Moghimi, and A. Rostami, "Linear and nonlinear superimposed Bragg grating: A novel proposal for all-optical multi-wavelength filtering and switching," *Progress In Electromagnetics Research*, Vol. 77, 243–266, 2007.
21. Jain, K., R. Mehra, and P. H. K. Dixit, "Optimization of 2×2 Mach-Zehnder interferometer electro-optic switch," *3th Int. Conf. on Computer and Communication Technology*, 171–174, 2012.
22. Skirtach, A. G., S. A. Boothroyd, and C. P. Grover, "Measurement of the nonlinear response in a strongly pumped erbium doped amplifiers for all-optical switching," *Proc. OFC'99*, 279–281, 1999.
23. Yakshin, M. A., C. R. Prasad, G. Schwemmer, M. Banta, and I. H. Hwang, "Compact, diode-pumped Yb : YAG laser with combination acousto-optic and passive Q-switch for LIDAR applications," *OSA/CLEO*, 1–2, 2011.
24. Kurumida, J. and S. J. B. Yoo, "Nonlinear optical signal processing in optical packet switching systems," *IEEE J. Quantum Electron.*, Vol. 18, 978–987, 2012.
25. Khorrami, Y., V. Ahmadi, and M. Razaghi, "Tb/s all-optical nonlinear switching using semiconductor optical amplifier based Mach-Zehnder interferometer," *20th Iranian Conference on Electrical Engineering (ICEE 2012)*, 118–123, Tehran, Iran, 2012.
26. Aboujeib, J., A. Pérennou, V. Quintard, and J. L. Bihan, "Evaluation of the crosstalk and losses in a multi-transducer acousto-optic switch," *3rd IEEE Int. Conf. Information and Communications Technologies: From Theory to Application (ICTTA'08)*, 1–6, Damascus, Apr. 7–11, 2008.
27. Ma, X. and G.-S. Kuo, "Optical switching technology comparison: Optical MEMS vs. other technologies," *IEEE Commun. Mag.*, Vol. 41, S16–S23, 2003.

28. Chen, D. and L. Shen, "Highly birefringent elliptical-hole photonic crystal fibers with double defect," *J. Lightwave Technol.*, Vol. 25, 2700–2705, 2007.
29. Chen, D., M.-L. Vincent Tse, and H.-Y. Tam, "Super-lattice structure photonic crystal fiber," *Progress In Electromagnetics Research M*, Vol. 11, 53–64, 2010.
30. Chen, D., G. Hu, X. A. Liu, B. Peng, and G. Wu, "Bending analysis of a dual-core photonic crystal fiber," *Progress In Electromagnetics Research*, Vol. 120, 293–307, 2011.
31. Khan, K. R., S. Bidnyk, and T. J. Hall, "Tunable all optical switch implemented in a liquid crystal filled dual-core photonic crystal fiber," *Progress In Electromagnetics Research M*, Vol. 22, 179–189, 2012.
32. Chen, D., M.-L. V. Tse, C. Wu, H. Y. Fu, and H. Y. Tam, "Highly birefringent four-hole fiber for pressure sensing," *Progress In Electromagnetics Research*, Vol. 114, 145–158, 2011.
33. Wu, J.-J., D. Chen, K.-L. Liao, T.-J. Yang, and W.-L. Ouyang, "The optical properties of Bragg fiber with a fiber core of 2-dimension elliptical-hole photonic crystal structure," *Progress In Electromagnetics Research Letters*, Vol. 10, 87–95, 2009.
34. Chau, Y.-F., C.-Y. Liu, H.-H. Yeh, and D. P. Tsai, "A comparative study of high birefringence and low confinement loss photonic crystal fiber employing elliptical air holes in fiber cladding with tetragonal lattice," *Progress In Electromagnetics Research B*, Vol. 22, 39–52, 2010.
35. Chen, D. and L. Shen, "Ultrahigh birefringent photonic crystal fiber with ultralow confinement loss," *IEEE Photon. Technol. Lett.*, Vol. 19, 185–187, 2007.
36. Beltrán-Mejía, F., G. Chesini, E. Silvestre, A. K. George, J. C. Knight, and C. M. B. Cordeiro, "Ultrahigh-birefringent squeezed lattice photonic crystal fiber with rotated elliptical air holes," *Opt. Lett.*, Vol. 35, 544–546, 2010.
37. Saitoh, K. and M. Koshiba, "Chromatic dispersion control in photonic crystal fibers: Application to ultra-flattened dispersion," *Opt. Express*, Vol. 11, 843–852, 2004.
38. Nozhat, N. and N. Granpayeh, "Specialty fibers designed by photonic crystals," *Progress In Electromagnetics Research*, Vol. 99, 225–244, 2009.
39. Chen, D., M.-L. Vincent Tse, and H.-Y. Tam, "Optical properties of photonic crystal fibers with a fiber core of arrays of subwavelength circular air holes: Birefringence and dispersion,"

Progress In Electromagnetics Research, Vol. 105, 193–212, 2010.

40. Singh, V. and D. Kumar, "Modal dispersion characteristics of a Bragg fiber having plasma in the cladding regions," *Progress In Electromagnetics Research*, Vol. 89, 167–181, 2009.
41. Huttunen, A. and P. Törmä, "Optimization of dual-core and microstructure fiber geometries for dispersion compensation and large mode area," *Opt. Express*, Vol. 13, 627–635, 2005.
42. Yang, S., Y. Zhang, X. Peng, Y. Lu, S. Xie, J. Li, W. Chen, Z. Jiang, J. Peng, and H. Li, "Theoretical study and experimental fabrication of high negative dispersion photonic crystal fiber with large area mode field," *Opt. Express*, Vol. 14, 3015–3023, 2006.
43. Knight, J. C. and D. V. Skryabin, "Nonlinear waveguide optics and photonic crystal fibers," *Opt. Express*, Vol. 15, 15365–15376, 2007.
44. Shen, G.-F., X.-M. Zhang, H. Chi, and X.-F. Jin, "Microwave/millimeter-wave generation using multi-wavelength photonic crystal fiber Brillouin laser," *Progress In Electromagnetics Research*, Vol. 80, 307–320, 2008.
45. Briks, T. A., J. C. Knight, and P. St. J. Russel, "Endlessly single-mode photonic crystal fiber," *Opt. Lett.*, Vol. 22, 961–963, 1997.
46. Lian, Z., P. Horak, X. Feng, L. Xiao, K. Frampton, N. White, J. A. Tucknott, H. Rutt, D. N. Payne, W. Stewart, and W. H. Loh, "Nanomechanical optical fiber," *Opt. Express*, Vol. 20, 29386–29394, 2012.
47. Szpulak, M., T. Martynkien, and W. Urbanczyk, "Effects of hydrostatic pressure on phase and group modal birefringence in microstructured holey fibers," *Appl. Opt.*, Vol. 43, 4739–4744, 2004.
48. Wu, C., B. O. Guan, Z. Wang, and X. Feng, "Characterization of pressure response of Bragg gratings in grapefruit microstructured fibers," *J. Lightwave Technol.*, Vol. 28, 1392–1397, 2010.
49. Huang, W. P., "Coupled-mode theory for optical waveguides: An overview," *J. Opt. Soc. Am. A*, Vol. 11, 963–983, 1994.
50. Nogueira, R. N., I. Abe, A. J. Fernandes, H. J. Kalinowski, J. R. F. da Rocha, and J. L. Pinto, "Spatial characterization of fiber Bragg grating structures using transversal pressure," *Optics Communications*, Vol. 259, 110–114, 2006.
51. Xie, H. M., P. Dabkiewicz, R. Ulrich, and K. Okamoto, "Side-hole fiber for fiber-optic pressure sensing," *Opt. Lett.*, Vol. 11, 333–335, 1986.